Geomechanics and Engineering, *Vol. 29, No. 2 (2022) 133-143*
https://doi.org/10.12989/gae.2022.29.2.133

Shaking table tests on the seismic response of slopes to near-fault ground motion

Chongqiang Zhu[1], Hualin Cheng[1], Yangjuan Bao[1,3], Zhiyi Chen[1,2] and Yu Huang*[1,2]

[1]*Department of Geotechnical Engineering, College of Civil Engineering, Tongji University, Shanghai 200092, China*
[2]*Key Laboratory of Geotechnical and Underground Engineering of the Ministry of Education, Tongji University, Shanghai 200092, China*
[3]*Department of Civil Engineering, Shanghai University, Shanghai 200444, China*

(Received July 28, 2020, Revised February 14, 2022, Accepted February 21, 2022)

Abstract. The catastrophic earthquake-induced failure of slopes concentrically distributed at near-fault area, which indicated the special features of near-fault ground motions, i.e. horizontal pulse-like motion and large vertical component, should have great effect on these geo-disasters. We performed shaking table tests to investigate the effect of both horizontal pulse-like motion and vertical component on dynamic response of slope. Both unidirectional (i.e., horizontal or vertical motions) and bidirectional (i.e., horizontal and vertical components) motions are applied to soft rock slope model, and acceleration at different locations is reordered. The results show that the horizontal acceleration amplification factor (AAF) increases with height. Moreover, the horizontal AAF under unidirectional horizontal pulse-like excitations is larger than that subject to ordinary motion. The vertical AAF does not show an elevation amplification effect. The seismic response of slope under different bidirectional excitations is also different: (1) The horizontal AAF is roughly constant under horizontal pulse-like excitations with and without vertical waves, but (2) the horizontal AAF under ordinary bidirectional ground motions is larger than that under unidirectional ordinary motion. Above phenomena indicate that vertical component has limited effect on seismic response when the horizontal component is pulse-like ground motion, but it can greatly enhance seismic response of slope under ordinary horizontal motion. Moreover, the vertical AAF is enhanced by horizontal motion in both horizontal pulse-like and ordinary motion. Thence, we should pay enough attention to vertical ground motion, especially its horizontal component is ordinary ground motion.

Keywords: near fault; pulse-like ground motion; seismic response; shaking table tests; vertical ground motion

1. Introduction

Earthquake-induced slope failure can cause massive casualties and economic losses and is one of the most common and serious geo-disasters worldwide. Hence, scholars have focused on earthquake-induced slope failure for decades to study their characteristics (Harp and Jibson 1996, Keefer 1984, Rodrıǵ uez *et al.* 1999). Field investigations have shown that earthquake-triggered landslides are concentratedly distributed in near-fault regions (Huang and Li 2009, Gorum *et al*. 2011, Zheng *et al.* 2012), which are generally referred to areas less than 20 km from the ruptured fault (Bray and Rodriguez-Marek 2004, Mazza *et al*. 2017). Landslides caused by the Wenchuan earthquake were distributed along the seismic fault and nearly 80% occurred in the near-fault region (Xu *et al.* 2014, Zhang *et al.* 2019). This suggests that seismic-induced slope failure should be strongly affected by certain features of near-fault waves.

Strong seismic records reveal that near-fault ground motion typically features pulse-like motion and a large vertical component (Davoodi *et al.* 2013, Wen *et al*. 2010, Mazza *et al.* 2017). Near-fault ground motion is often significantly affected by forward directivity and fling-steps, exhibiting long-period pulses and high peak velocities (Somerville *et al.* 1997, Bray and Rodriguez-Marek 2004). Hence, near-fault pulse-like ground motion usually presents high intensities with concentrated seismic energy in the pulse, which can push structures and slopes into the inelastic and non-linear region (Song and Rodriguez-Marek, 2015) and lead to considerably more serious damage than ordinary ground motion (Bhattacharya *et al.* 2018, Liu *et al.* 2021). Another prominent feature of near-fault seismic waves is the peak ground acceleration (PGA) of the vertical component, which can be equal to or larger than that of the horizontal component (Yin 2014, Wen *et al.* 2010). For example, the PGA of the horizontal and vertical acceleration records observed at the Wolong station during the 2008 Wenchuan earthquake were nearly the same (0.957 g and 0.948 g, respectively), whereas the PGA recorded at the Bajiao station was larger in the vertical direction (0.650 g) than in the horizontal direction (0.590 g). However, in previous analyses of seismic slope stability, vertical ground motion has been often neglected or only assumed to be 2/3 of the horizontal ground motion in seismic design (Wen *et al*. 2010), which may lead to an underprediction of the seismic disaster in a near-fault region. Because of the salient aforementioned features, near-fault ground motion can lead to strong seismic demands on slopes and hence

*Corresponding author, Professor
E-mail: yhuang@tongji.edu.cn

ISSN: 2005-307X (Print), 2092-6219 (Online)

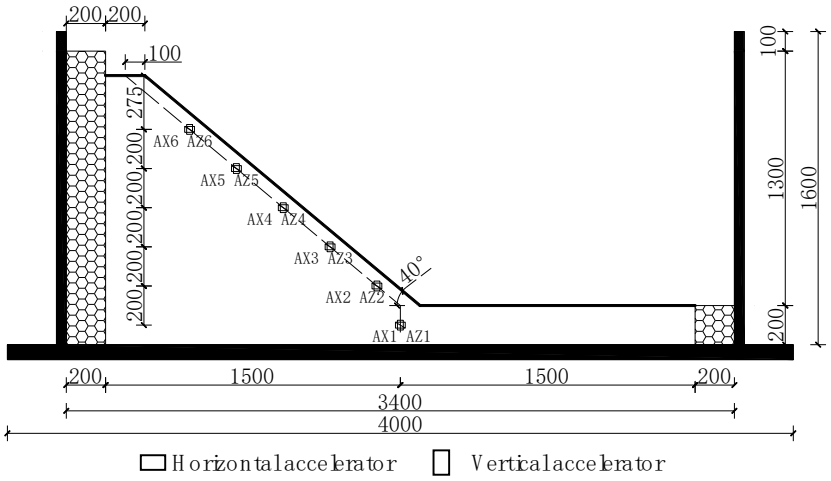

Fig. 1 Layout of the shaking table tests and instrumentation (units: mm)

pose a great challenge in seismic slope stability assessment.

Shaking table tests based on a strict similitude design can directly model the dynamic performance of slopes subject to seismic activity and are therefore widely used to investigate slope seismic response. Wang and Lin (2011) studied the initiation and failure of earthquake-triggered landslides based on shaking table tests. The criteria for identifying initiation and failure are well defined by analyzing shaking table results. The seismic stability of slopes and influence of lithology and structure were investigated using shaking table tests (Liu *et al.* 2014). Elevation amplification effects, which is that the peak acceleration of the slope is larger than input motion and also increases with the elevation, were observed in all cases and soft-rock slopes presented considerably more serious responses under seismic loading than those of hard-rock slopes. Yang *et al.* (2018) studied the seismic response and deformation features of an anti-slope under sine waves and field ground motion. The effect of slope type (steep-bedding vs. toppling) and input ground motion on seismic response has been investigated and different failure mechanisms for different slope type have been compared (Li *et al*. 2019). Wu *et al*. (2020) studied the seismic response and deformation evolution of loess slopes with and without fissures and concluded that fissured loss slopes present more bond failure. Moreover, shaking table tests are slope adopted to evaluate dynamic properties of residual soils (Lim *et al*. 2018), seismic responses of reinforced soil retaining walls (Panah *et al*. 2015), soil liquefaction induced by cyclic loading (Molina-Gomez *et al.* 2019) and performance of geogrid (Zarnani *et al.* 2011). These previous studies demonstrate that the seismic response of slopes can be effectively investigated using shaking table tests. However, the response of slopes subject to near-fault ground motion from shaking table tests has not been reported. With the development of numerical algorithm and computer hardware, seismic response of slope or site was well studied using advanced numerical tools by considering complex topographic and stratigraphic effects and geotechnical characteristics in previous works (Bouckovalas and Papadimitriou 2005, Falcone *et al*. 2020, 2018, Gatmiri and Arson 2008, Jin *et al*. 2021, Rizzitano *et al.* 2014), especially the work conducted by Jin *et al*. (2021), in which the numerical and experimental (i.e., 1 g shaking table) were compared and good agreement was presented. These research achievements have great potential to provide guidelines for seismic risk evaluation and mitigation. However, most of these numerical findings except these in Jin *et al*. (2021) are lack of experimental or field data for comparison and validation, which has limited their application in real engineering projects. The huge demand for experimental data further confirms the significance of shaking table tests.

In this work, we performed shaking table tests to evaluate the impact of certain characteristics of near-fault ground motion (pulse-like features, large vertical component) on the seismic response of slopes. The seismic performance of slopes under different seismic excitations was recorded using horizontal and vertical acceleration sensors. The results of this study provide insight on the seismic response of slopes in near-fault areas and demonstrate the importance of seismic design development for slopes in these regions.

2. Experimental design

2.1 Experimental equipment and model box

The shaking table tests were performed using a large-scale MTS shaking table device developed at the State Key Laboratory for Disaster Reduction in Civil Engineering, Tongji University. The shaking table is a three-dimensional facility with six degrees of freedom that can generate three-dimensional vibrations. The table dimensions are 4.0 × 4.0 m, the capacity is 25 t, the operating frequency is 0.1–50 Hz, and the maximum velocity is 1000 mm/s in the *X*-direction and 600 mm/s in the *Y*- and *Z*-directions. The maximum acceleration under a load of 15 t (i.e., the load applied for the examined case studies) is 1.2 g, 0.8 g, and 0.7 g in the *X*-, *Y*-, and *Z*- directions, respectively.

A rigid model box with inner dimensions of 3.4 × 1.0 ×

Table 1 Scaling factors used in the shaking table tests

Physical quantity	Similarity relationship	Scale factor
Length (L)	C_L	25
Density (ρ)	C_ρ	1
Acceleration (a)	C_a	1
Modulus (M)	$C_M = C_L\, C_\rho\, C_a$	25
Cohesion (c)	$C_c = C_L\, C_\rho\, C_a$	25
Internal friction angle (φ)	C_φ	1
Poison's ratio (μ)	C_μ	1
Stress (σ)	$C_\sigma = C_L\, C_\rho\, C_a$	25
Time (t)	$C_t = C_L^{1/2}\, C_a^{-1/2}$	5
Velocity (v)	$C_v = C_L^{1/2}\, C_a^{1/2}$	5
Displacement (d)	$C_d = C_L$	25

1.6 m was used to study the dynamic responses of a slope under near-fault ground motion. The model box was rigidly mounted on the shaking table to ensure the vibration was exerted on the slope. To minimize boundary effects, a closed-hole polyethylene foam absorber was placed on both ends of the model box (Fig. 1) according to previous work (Lombardi *et al.* 2015).

2.2 Scaling factor design and model material

The scaling factors for the shaking table tests were determined based on similarity theory (Iai 1988) and are listed in Table 1. In this work, the scaling factors of geometry (length) C_L, density C_ρ, and acceleration C_a were selected as independent parameters. The geometric similitude C_L was set to 25 considering the maximum operating frequency of the shaking table. Both C_ρ and C_a were set to 1.0. The scaling factors of the other physical quantities, which can be calculated based on Buckingham's π theorem, are presented in Table 1.

To model soft-rock slope, we used barite powder, quartz sand, gypsum, glycerol, and water to prepare model material based on previous shaking table tests (Liu *et al*. 2014). Barite powder and quartz sand served as fine and coarse aggregates, respectively. Gypsum and water acted as cement. Glycerol was used to adjust the mixture strength. Massive uniaxial compression strength tests and direct shear tests were carried out based on standard geotechnical testing methods (GB/T 50123–2019) to determine material proportions. Model material with a weight ratio of 29.3:49.4:15:1.4:5.0 (barite powder: quartz sands: gypsum : glycerol : water) was used to model soft rock. The density, uniaxial compression strength, internal frictional angle, and cohesion of the model material were 1.80 g/cm^3, 0.77 MPa, 38.7°, and 54.65 kPa, respectively, which corresponds to prototypical properties of 1.80 g/cm^3, 19.25 MPa, 38.7°, and 1.36 MPa according to the scaling factors. Moreover, the compressional and shear wave velocities of model material were 1425 m/s and 755 m/s respectively in prototype scale (i.e., 285 m/s and 151 m/s in model scale), which were obtained by employing a Pundit Lab ultrasonic instrument provided by PROCEQ Ltd., Switzerland.

Table 2 Characteristics of the input ground motion

Information	Station	Date	PGA (g)	PGV (cm/s)	PGV/PGA (s)
MZQ-EW	Qingping	12/05/2008	0.824	138.40	0.171
MZQ-UD	Qingping	12/05/2008	0.623	39.57	0.065
WCW-EW	Wolong	12/05/2008	0.957	52.89	0.056
WCW-UD	Wolong	12/05/2008	0.948	24.97	0.027

2.3 Model setup

Fig. 1 shows the configuration of the model slope. Previous field investigations found that more than 80% of earthquake-induced landslides occurred on slopes with gradient ranges from 30° and 50° (Sun *et al.* 2015), and a slope of about 40° is most prone to failure subject to earthquake. Hence, we set the gradient of the model slope to 40°. The model slope was built using wet pour and compaction methods. The model materials were mixed according to above ratios and poured into the model box. Layered compaction was conducted to ensure the desired density. The thickness of each layer was 10 cm to maintain a homogenous model slope. Both the horizontal and vertical accelerometers were positioned to investigate the seismic response of the slope (Fig. 1).

3. Near-fault ground motion

The selection of suitable ground motion is important for investigating the dynamic response of slope under near-fault ground motion. Previous studies (Bouckovalas and Papadimitriou 2005, Rizzitano *et al*. 2014) found that the seismic response of soil slope can be affected by normalized frequency H/λ for slope height H and wavelength λ. Actually, the effect of H/λ will reduced to the effect of input motion frequency provided the slope keeps the same. To study frequency of motion, harmonic or nearly harmonic waves with narrow frequency distribution would be a good choice. However, we aim to study the effect of near-fault pulse-like motion and vertical component on seismic response of slope. Hence, the H/λ is not considered during selection of input waves. In this work, we adopt an index that is the ratio of peak ground velocity (PGV) to peak ground acceleration (PGA) to quantitively define pulse-like characteristics of near-fault waves. According to previous studies, pulse-like ground motion can be recognized when PGV/PGA > 0.15 (Bray and Rodriguez-Marek 2004, Loh *et al*. 2002). On basis of this criterion, the MZQ-EW ground motion with the highest PGV/PGA (0.171; Table 2) among the 2008 Wenchuan earthquake was selected from the database of the National Strong Motion Networks Center of China (http://www.smsd-iem.net.cn) as the near-fault pulse-like ground motion. To compare slope seismic responses, the WCW-EW ground motion, which is an ordinary seismic wave without pulse-like characteristics and widely used in geological engineering, was employed as control case. The acceleration and velocity time histories

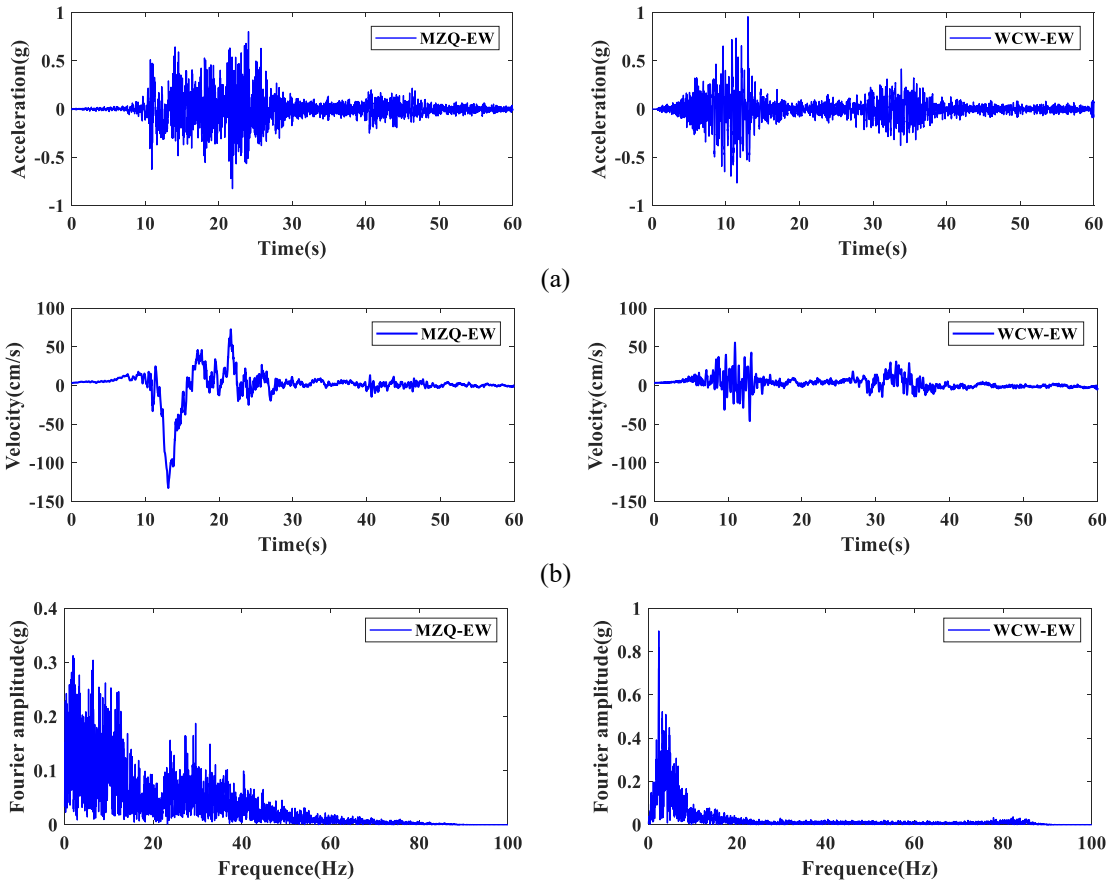

Fig. 2 Time history of acceleration (a), velocity (b) and Fourier amplitude spectrum (c) of recorded MZQ-EW and WCW-EW waves

and Fourier amplitude spectrum of both ground motions are presented in Fig. 2. Their corresponding vertical ground motion (Fig. 3), which are both ordinary ground motion, are used to investigate the seismic response of the slope under vertical ground motion.

Bearing in mind that the maximum acceleration under a load of 15 t is 1.2 g, 0.8 g, and 0.7 g in the X-, Y-, and Z-directions, respectively, and considering that deep-seated landslides are often induced by earthquakes with PGA of 0.5 g, determined based on detailed field surveying (Huang *et al*. 2017), the input ground motion (both horizontal and vertical components) was scaled down to 0.5 g. The PGA of all input motions keeps the same to remove the effect of PGA on seismic response of slopes. Moreover, the same PGA for both horizontal and vertical components can well simulate large vertical component observed in near fault area, where the vertical PGA is always equal or larger than horizontal PGA (Wen *et al*. 2010). Both unidirectional (i.e., horizontal or vertical motion) and bidirectional ground motions (i.e., horizontal and vertical components) were applied to the model slope to study the seismic response. The test cases are listed in Table 3. To ensure the slope model keep nearly same condition during each seismic wave, the white is applied before and after seismic waves (i.e., case 1 and 8). Nearly similar response of slope for case 1 and 8 confirmed that different seismic response of slope was induced by input motion.

Table 3 Shaking table test conditions

Cases	Ground motion
1	White Noise
2	WCW-EW
3	WCW-UD
4	MZQ-UD
5	MZQ-EW
6	WCW-EW-UD
7	MZQ-EW-UD
8	White Noise

4. Results and discussion

The following experimental results are described at a prototype scale without specification.

4.1 Slope seismic response under horizontal input motion

To investigate the impact of near-fault pulse-like waves on the seismic response of a slope, we separately input horizontal ground motion of MZQ-EW and WCW-EW, whose peak accelerations were adjusted to 0.5 g. The horizontal and vertical acceleration amplification factor

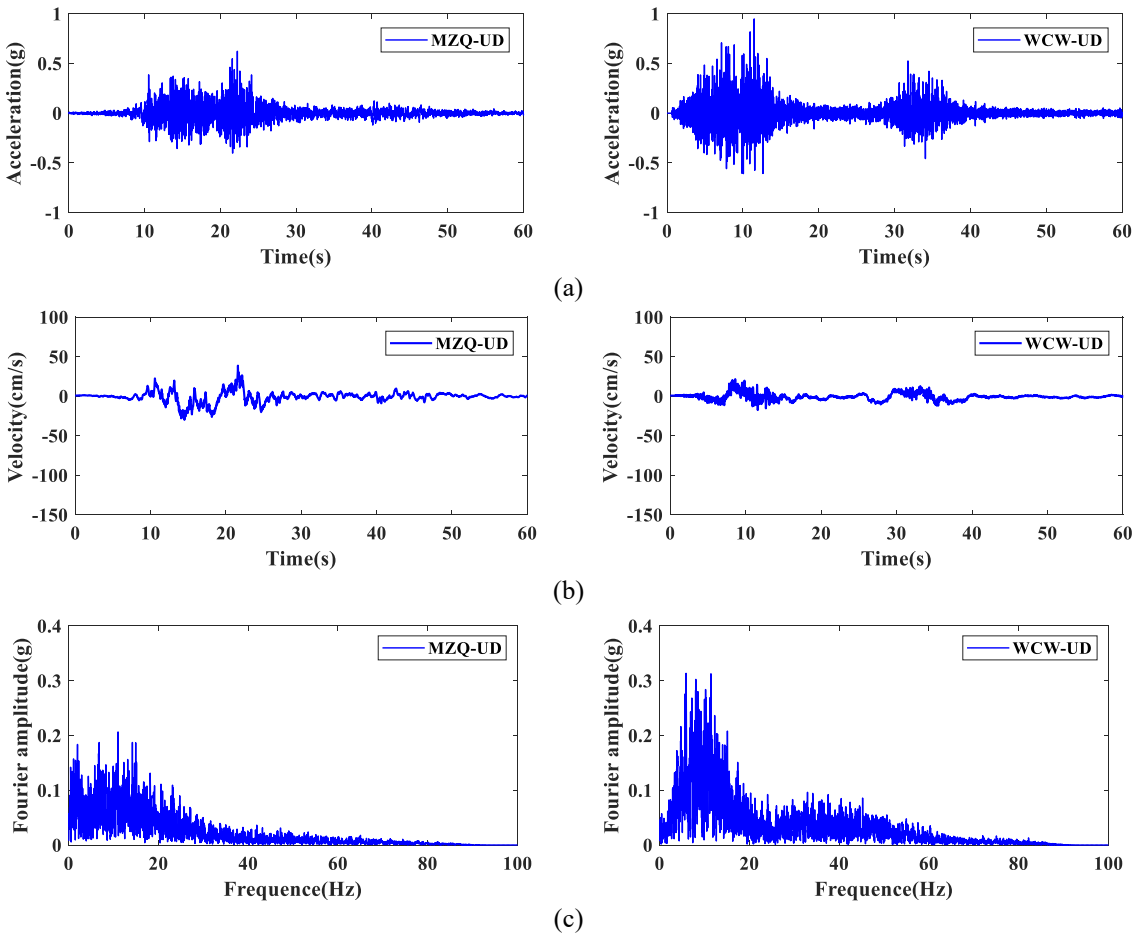

Fig. 3 Time history of acceleration (a), velocity (b) and Fourier amplitude spectrum (c) of recorded MZQ-UD and WCW-UD waves

(AAF) along the slope height is shown in Fig. 4. The AAF is the ratio of measured PGA to the PGA of the input motion, which is a widely used and recognized index to evaluate the seismic response of slopes. The red data points in Fig. 4 show the AAF profile of a slope subject to WCW-EW ground motion, and the blue data points shows the results under MZQ-EW ground motion. The horizontal AAF (Fig. 4(a)) increases with height in both cases, which is a typical elevation amplification effect. The elevation amplification effect has been observed in previous field surveys and shaking table tests (Huang and Li 2009, Liu *et al.* 2014), which indicates that the setup of our shaking table tests is appropriate and the experimental data are reliable. Although the same trend is observed, the horizontal AAF at same height presents salient differences in the different cases. Specifically, the horizontal AAF subject to pulse-like waves is larger than that at the same height under ordinary ground motion. Moreover, the difference increases with height and reaches 1.3 at the height of 27.5 m. The vertical AAF, which is the ratio measured PGA in vertical direction to the input PGA of horizontal motion for cases under unidirectional horizontal motion, is shown in Fig. 4(b). The parasitic vertical acceleration is induced by the complex slope-horizontal motion interaction, which has been well studied in previous papers by means of numerical simulation of local seismic site response (Bouckovalas and Papadimitriou 2005, Rizzitano *et al.* 2014). The vertical AAF is roughly constant across whole height in both cases. But the vertical AAF under pulse-like wave (i.e., blue line in Fig. 4(b)) is larger than that under ordinary motion (i.e., red line), which presents similar trend with horizontal AFF. Higher AAF in both horizontal and vertical directions under pulse-like motion means that more serious damage can occur along slopes under near-fault pulse-like ground motion. This implies that near-fault pulse-like waves are more destructive than ordinary ground motion.

We explore the mechanism of increased seismic response of the slope as follows. Although both the PGA of pulse-like and ordinary ground motion was set to 0.5 g, the seismic energy contained under different ground motion types substantially differ. The Arias intensity (Arias 1970) refers to the integration of the square of ground motion over time, which depicts the accumulated energy of the unit weight obtained by infinite single-degree-of-freedom oscillators and has been proven to be a fairly reliable index for measuring ground motion energy (Liu *et al.* 2016, Zhang *et al.* 2019). Hence, we select the Arias intensity to represent the energy carried by ground motion. The Arias intensity is 4.35 m/s and 2.83 m/s for the MZQ-EW and WCW-EW, respectively, when the PGA is 0.5 g. Pulse-like ground motion carries higher energy than ordinary ground motion. Hence, substantially more energy was applied to

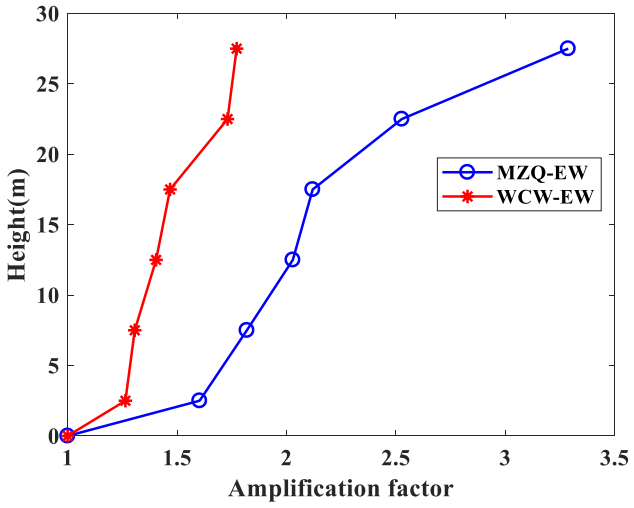

(a)

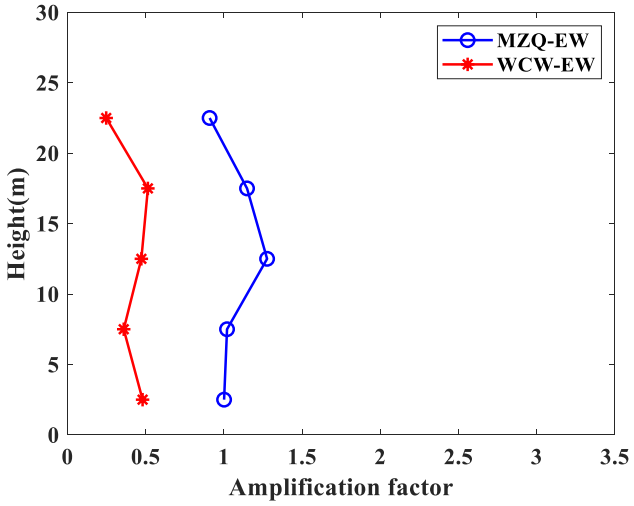

(b)

Fig. 4 Distribution of the horizontal (a) and vertical (b) AAF with slope height under unidirectional horizontal seismic waves

the slope system by pulse-like ground motion, which results in the increased seismic response. This provides a rational explanation for the occurrence of large landslides around near-fault areas. It also demonstrates that the PGV, velocity time history, and energy of seismic waves should be considered and not only PGA when conducting earthquake-induced landslide hazard analysis over large areas (Del Gaudio *et al*. 2012, Mori *et al*. 2020, Nowicki Jessee *et al.* 2018).

The normalized frequency (or normalised wavelength) H/λ is used to investigate the effect frequency of motion on seismic response and some useful conclusions have been reported in previous papers (Bouckovalas and Papadimitriou 2005, Rizzitano *et al*. 2014). However, we cannot directly compare our data with these results considering the following differences: (1) Different influencing factors. This part is focus on horizontal pulse-like motion instead of frequency, while previous studies are to investigate the effect of frequency. (2) Different definition of the AAF. The AAF is the ratio of measured PAG to the PGA of input motion in this work. But the AAF is the ratio of measured PAG to the PGA recorded in free field (Bouckovalas and Papadimitriou 2005, Rizzitano *et al.* 2014). (3) Different material. The material of our slope model is soft rock, while their material is soil. We thus cannot compare our data with the previous research. However, the H/λ should be considered when we study the effect of pulse period in the future.

4.2 Seismic response under vertical input motion

Earthquakes can generate multi-dimensional vibrations. However, the seismic design of slopes often focuses on horizontal ground motion and ignores vertical ground motion. Recent field investigations and numerical studies have shown that vertical ground motion exerts a strong effect on the seismic responses of slopes, especially for slopes located in near-fault areas (Yin 2014, Sun *et al.* 2012, Zhang *et al.* 2015). We designed unidirectional and bidirectional excitation cases to determine the impacts of

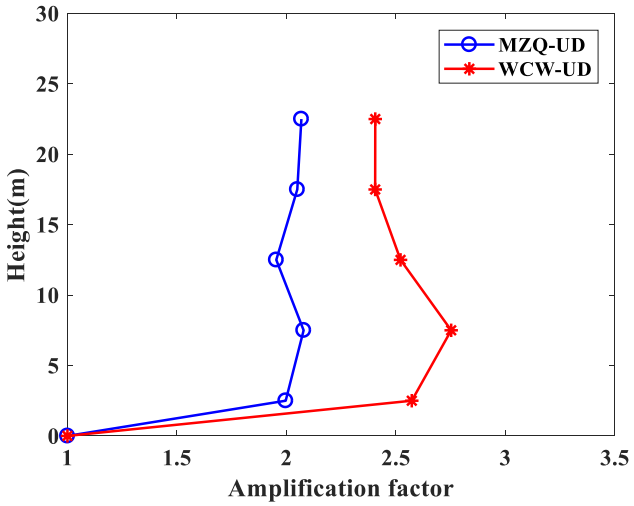

Fig. 5 Distribution of the vertical acceleration amplification factor with slope height under vertical seismic waves

bidirectional ground motion on the slope dynamic response.

The PGA of both the horizontal and vertical ground motions was adjusted to 0.5 g considering that the vertical component is often equal to or greater than the horizontal component in near-fault regions. Although the ratio of PGA_UD/PGA_EW is 0.76 for MZQ motion, it is still larger than 2/3 which is often assumed ratio in seismic design (Wen *et al*. 2010). The MZQ-UD thus belongs to large vertical component. The seismic response of slopes under unidirectional horizontal ground motion is discussed in section 4.1. The AAF profile of a slope subject to unidirectional vertical ground motion is presented in Fig. 5.

The blue data points show the results under MZQ-UD ground motion. The AAF is around 2.0, which means that vibrations were amplified in the slope. However, the results do not present a clear elevation amplification effect, which has been observed in cases under unidirectional horizontal ground motion. The seismic response of slopes under WCW-UD presents a similar trend with slight differences. The AAF increases from the ground to a height of 7.5 m; however, it then decreases with increasing height to 22.5 m. The amplification was definite because all of the AAF were larger than 1.0. Moreover, the AAF under the WCW-UD wave are larger than that subject to the MZQ-UD wave, which means that WCW-UD ground motion can lead to more serious damage to the model slope than MZQ-UD ground motion. Because the two vertical motions are both ordinary motions without pulse-like features, we thus ignore the effect of PGV due to small value (i.e., 0.31 and 0.12 m/s for MZQ-UD and WCW-UD respectively) on seismic response. The Arias Intensity of MZQ-UD and WCW-UD is 2.90 m/s and 3.60 m/s respectively when PGA is 0.5 g. Larger AAF under WCW-UD which has larger Arias Intensity was also observed. This phenomenon reconfirms the correlation between Arias Intensity and AAF.

4.3 Seismic response under horizontal and vertical input motions

The seismic responses of the model slope subject to bidirectional WCW-EW-UD ground motion and MZQ-EW-UD waves are presented separately in Figs. 6 and 7. The horizontal AAF under WCW-EW-UD ground motion (blue data points in Fig. 6(a)) shows an evident elevation amplification effect. The horizontal AAF under bidirectional WCW excitations is clearly larger than that under unidirectional vibration except at the height of 2.5 m.

The difference increases with height and reaches 1.1 at the height of 27.5 m, which means that substantially more damage occurred in the model slope under bidirectional vibrations. We can thus conclude that vertical ground motion can strongly enhance the seismic response of slopes, which indicates that more attention should be paid to multi-directional excitation instead of to only unidirectional horizontal vibration when conducting dynamic slope performance analysis. The vertical AAF profiles under unidirectional and bidirectional excitations, presented in Fig. 6b, show similar trends but different amplitudes. The vertical AAF under WCW-EW-UD ground motion (blue data points) is larger than that under unidirectional horizontal (green data points) and vertical (red data points) excitation. This phenomenon also confirms that the seismic response of the model slope in the vertical direction is enhanced by horizontal ground motion.

The horizontal AAF of the model slope subject to MZQ-EW-UD is shown as red data points in Fig. 7(a). The elevation amplification effect of the horizontal AAF is clearly recorded under bidirectional excitations. However, the horizontal AAF under bidirectional excitation is nearly the same as that under unidirectional horizontal vibration and slightly decreases at the height of 7.5 m and 12.5 m monitoring points. Hence, the vertical component only has a limited effect on the dynamic response when the slope is subject to pulse-like ground motion. However, the vertical AAF under bidirectional excitation (red data points) is higher than that under unidirectional horizontal (green data point) and vertical (blue data points) vibration, whereas the trend of the vertical AAF profile presents similar characteristics. The above analysis shows that the vertical component has a limited impact on the horizontal seismic

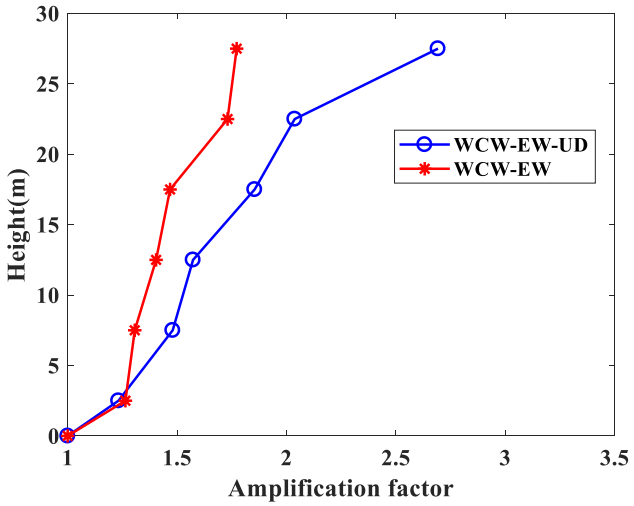

(a) Horizontal amplification

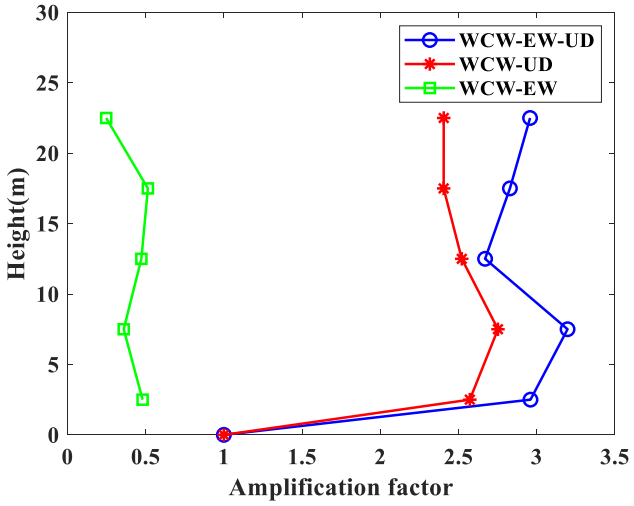

(b) Vertical amplification

Fig. 6 Distribution of the acceleration amplification factor with slope height under unidirectional and bidirectional WCW waves

response when the slope is under horizontal near-fault pulse-like ground motion, whereas the vertical seismic response is clearly enhanced by horizontal excitation.

Although the impact of vertical ground motion on the dynamic responses of slopes remains disputed based on numerical simulations (Gazetas *et al*. 2009, Sun *et al.* 2012, Zhang *et al*. 2015), our experimental results firmly indicate the importance of vertical ground motion, especially when the horizontal ground motion is ordinary waves in near-fault regions. Further research is required to determine the mechanism of the enhanced seismic response of slopes by vertical ground motion.

5. Conclusions

We performed large-scale shaking table tests to investigate the effects of near-fault ground motion (horizontal pulse-like motion and large vertical component) on the seismic response of slopes. The pulse-like motion is featured by prominent pulse for the time history of velocity and can be recognized using PGV/PGA. The large vertical component means that the PGA of vertical component of near fault motion is equal or even greater than the PGA of horizontal component, which is different from that the vertical PGA is assumed as 2/3 of the horizontal PAG in previous seismic design (Wen *et al.* 2010). The following main conclusions were drawn.

- For pulse-like motion. Our results show that near-fault pulse-like ground motion can strongly enhance the slope response. An elevation amplification effect is observed in all cases, which indicates the effectiveness and reliability of the experimental results. However, both the horizontal and vertical (parasitic vertical motion) AAF under unidirectional horizontal near-fault pulse-like waves is greater than that subject to ordinary earthquake wave with the same PGA. The enhanced seismic response may be caused by the high energy of near-fault pulse-like ground motion.

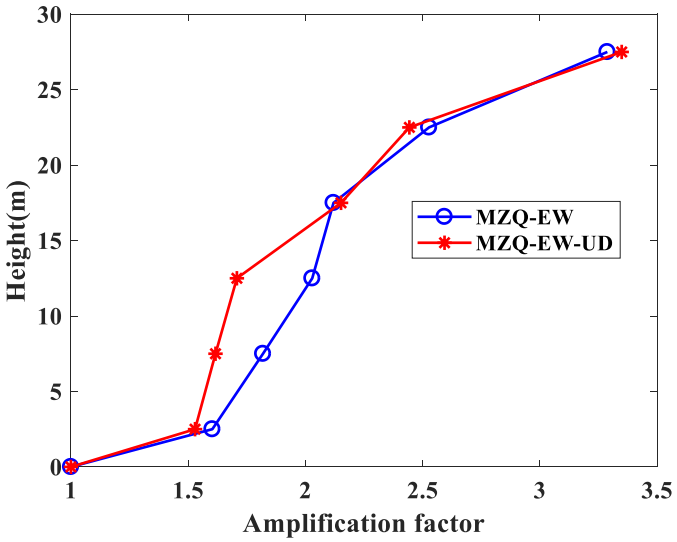

(a) Horizontal amplification

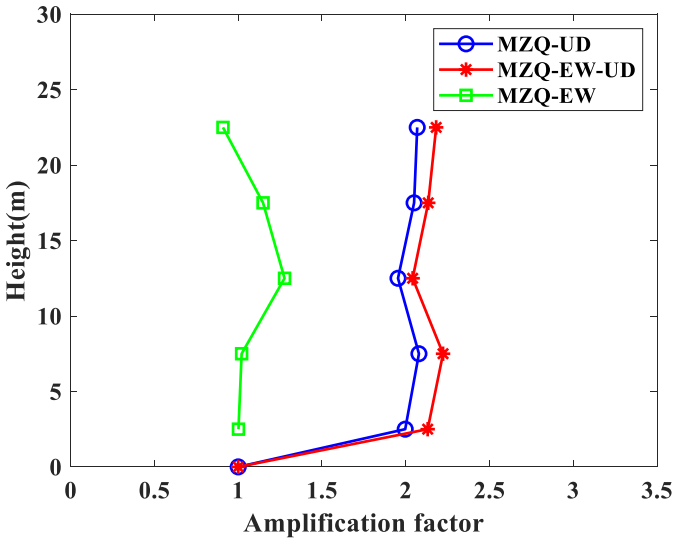

(b) Vertical amplification

Fig. 7 Distribution of the acceleration amplification factor with slope height under unidirectional and bidirectional MZQ waves

• For vertical motion. Differed from horizontal AAF, the vertical seismic response of the slope does not show an elevation amplification effect. The vertical seismic response of the slope is greatly enhanced by horizontal component. However, the impact of the vertical component on slope horizontal dynamic response differs for different cases. When the horizontal motion is pulse-like motion, the effect of vertical component on horizontal AAF of slope is limited. However, the vertical component can strongly enhance the horizontal AAF of slope when ordinary horizontal ground motion is applied. Although the mechanism requires further study, the results presented here imply that sufficient attention must be paid to vertical ground motion during seismic design, especially for cases under ordinary ground motion in near-fault areas.

Finally, we note that this work preliminarily reveals the complex effect of pulse-like motion and vertical component on seismic response of slope, serving as an initial step to understand the slope failure under near-fault ground motion. It is promising and interesting to conduct further research to investigate the effect of pulse period (e.g., using H/λ), the PGV/PGA ratio, the PGA_UD/PGA_EW ratio, etc. on the seismic responses of slopes in the future work.

Acknowledgments

This work was supported by the National Natural Science Foundation of China (Grant Nos. 41625011 and 51808401), the China Postdoctoral Science Foundation (Grant Nos. 2017M620167 and 2020T130472), and the Fundamental Research Funds for the Central Universities. The records used in this work are provided by the National

Strong Motion Networks Center of China (http://www.smsd-iem.net.cn).

References

Arias, A. (1970), A Measure of Earthquake Intensity. In Seismic Design for Nuclear Power Plants. Massachusetts Institute of Technology Press, Cambridge, UK.

Bhattacharya, S., Hyodo, M., Nikitas, G., Ismael, B., Suzuki, H., Lombard, D., Egami, S., Watanabeb, G. and Goda, K. (2018), "Geotechnical and infrastructural damage due to the 2016 Kumamoto earthquake sequence", *Soil Dyn. Earthq. Eng*., **104**, 390-394. https://doi.org/10.1016/j.soildyn.2017.11.009.

Bouckovalas, G.D. and Papadimitriou, A.G. (2005), "Numerical evaluation of slope topography effects on seismic ground motion", *Soil Dyn. Earthq. Eng*., **25**, 547-558. https://doi.org/10.1016/j.soildyn.2004.11.008

Bray, J.D. and Rodriguez-Marek, A. (2004), "Characterization of forward-directivity ground motions in the near-fault region", *Soil Dyn. Earthq. Eng*., **24**(11), 815-828. https://doi.org/10.1016%2Fj.soildyn.2004.05.001

Davoodi, M., Jafari, M.K. and Hadiani, N (2013), "Seismic response of embankment dams under near-fault and far-field ground motion excitation", *Eng. Geol*., **158**, 66-76. https://doi.org/10.1016%2Fj.enggeo.2013.02.008.

Del Gaudio, V., Pierri, P. and Calcagnile, G. (2012), "Analysis of seismic hazard in landslide-prone regions: criteria and example for an area of Daunia (southern Italy)", *Nat. Hazards*, **61**(1), 203-215. https://doi.org/10.1007/s11069-011-9886-5.

Falcone, G., Boldini, D. and Amorosi, A. (2018), "Site response analysis of an urban area: A multi-dimensional and non-linear approach", *Soil Dyn. Earthq. Eng*., **109**, 33-45. https://doi.org/10.1016/J.SOILDYN.2018.02.026.

Falcone, G., Boldini, D., Martelli, L. and Amorosi, A. (2020), "Quantifying local seismic amplification from regional charts and site specific numerical analyses: a case study". *Bull. Earthq. Eng.*, **18**, 77-107. https://doi.org/10.1007/s10518-019-00719-9.

Gatmiri, B. and Arson, C. (2008), "Seismic site effects by an optimized 2D BE/FE method II. Quantification of site effects in two-dimensional sedimentary valleys". *Soil Dyn. Earthq. Eng*., **28**, 646-661. https://doi.org/10.1016/J.SOILDYN.2007.09.002.

Gazetas, G., Garini, E., Anastasopoulos, I. and Georgarakos, T. (2009), "Effects of near-fault ground shaking on sliding systems". *J. Geotech. Geoenviron. Eng.*, **135**(12), 1906-1921. https://doi.org/10.1061%2F%28asce%29gt.1943-5606.0000174.

Gorum, T., Fan, X., van Westen, C.J., Huang, R.Q., Xu, Q., Tang, C. and Wang G (2011), "Distribution pattern of earthquake-induced landslides triggered by the 12 May 2008 Wenchuan earthquake", *Geomorphology*, **133**(3-4), 152-167. https://doi.org/10.1016%2Fj.geomorph.2010.12.030.

Harp, E.L. and Jibson, R.W. (1996), "Landslides triggered by the 1994 Northridge, California, earthquake", *Bull. Seismol. Soc. Am.*, **86.1B**, 319-332. https://doi.org/10.1785/BSSA08601BS319

Huang, M.H., Fielding, E.J., Liang, C., Milillo, P., Bekaert, D., Dreger, D. and Salzer, J. (2017), "Coseismic deformation and triggered landslides of the 2016 Mw 6.2 Amatrice earthquake in Italy", *Geophys. Res. Lett.*, **44**(3), 1266-1274. https://doi.org/10.1002%2F2016gl071687.

Huang, R.Q. and Li, W.L. (2009), "Analysis of the geo-hazards triggered by the 12 May 2008 Wenchuan Earthquake, China", *Bull. Eng. Geol. Environ*., **68**(3), 363-371. https://doi.org/10.1007%2Fs10064-009-0207-0.

Iai, S. (1988), "Similitude for shaking table tests on soil-structure-fluid model in 1 g gravitational field", *Rep. Port Harb. Res. Inst. Minist. Transp. Jpn.*, **27** (3), 1-24.

Jin, Y., Kim, H., Kim, D, Lee, Y. and Kim, H. (2021), "Seismic response of flat ground and slope models through 1 g shaking table tests and numerical analysis". *Appl. Sci*., **11**, 1-20. https://doi.org/10.3390/app11041875.

Keefer, D.K. (1984), "Landslides caused by earthquakes", *Geol. Soc. Am. Bull.*, **95**, 406-421. https://doi.org/10.1130/0016-7606(1984)95<406:LCBE>2.0.CO;2.

Li, L.Q., Ju, N.P., Zhang, S. and Deng, X.X. (2019), "Shaking table test to assess seismic response differences between steep bedding and toppling rock slopes", *Bull. Eng. Geol. Environ*., **78**(1), 519-531. https://doi.org/10.1007%2Fs10064-017-1186-1

Liu, J., Zhang, Y., Wei, J., Xian, C., Wan, Q., Xu, P. and Fu, H. (2021), "Hazard assessment of earthquake-induced landslides by using permanent displacement model considering near-fault pulse-like ground motions", *Bull. Eng. Geol. Environ*., 1-16. https://doi.org/10.1007/s10064-021-02464-3.

Lim, J.X., Lee, M.L. and Tanaka, Y. (2018), "1 g shaking table tests on residual soils in Malaysia through different model setups", *Geomech. Eng*., **16**(5), 547-558. https://doi.org/10.12989/gae.2018.16.5.547.

Liu, H.X., Xu, Q. and Li, Y.R. (2014), "Effect of lithology and structure on seismic response of steep slope in a shaking table test". *J. Mt. Sci.*, **11**(2), 371-383. https://doi.org/10.1007%2Fs11629-013-2790-6.

Liu, J.M., Wang, T., Wu, S.R. and Gao, M.T. (2016), "New empirical relationships between Arias intensity and peak ground acceleration", *Bull. Seismol. Soc. Am*., **106**(5), 2168-2176. https://doi.org/10.1785%2F0120150366.

Loh, C.H., Wan, S. and Liao, W.I. (2002), "Effects of hysteretic model on seismic demands: consideration of near-fault ground motions", *Struct. Des. Tall Build*., **11**(3), 155-169. https://doi.org/10.1002%2Ftal.182.

Lombardi, D., Bhattacharya, S., Scarpa, F. and Bianchi, M. (2015), "Dynamic response of a geotechnical rigid model container with absorbing boundaries", *Soil Dyn. Earthq. Eng.*, **69**, 46-56. https://doi.org/10.1016%2Fj.soildyn.2014.09.008.

Mazza, F., Mazza, M. and Vulcano, A. (2017), "Nonlinear response of rc framed buildings retrofitted by different base-isolation systems under horizontal and vertical components of near-fault earthquakes", *Earthq. Struct.*, **12**(1), 135-144. https://doi.org/10.12989%2Feas.2017.12.1.135.

Molina-Gomez, F., Caicedo, B., Viana da Fonseca, A (2019), "Physical modelling of soil liquefaction in a novel micro shaking table", *Geomech. Eng.*, **19**(3), 229-240. https://doi.org/10.12989/gae.2019.19.3.229.

Mori, F., Gena, A., Mendicelli, A., Naso, G. and Spina, D. (2020), "Seismic emergency system evaluation: The role of seismic hazard and local effects", *Eng. Geol*., **270**, 105587. https://doi.org/10.1016/j.enggeo.2020.105587.

Nowicki Jessee, M.A., Hamburger, M.W., Allstadt, K., Wald, D.J., Robeson, S.M., Tanyas, H., Hearne, M. and Thompson, E.M. (2018), "A global empirical model for near-real-time assessment of seismically induced landslides", *J. Geophys. Res.: Earth Surf.*, **123**(8), 1835-1859. https://doi.org/10.1029/2017JF004494.

Panah, A.K., Yazdi. M. and Ghalandarzadeh, A. (2015), "Shaking table tests on soil retaining walls reinforced by polymeric strips". *Geotext. Geomembranes*, **43**(2), 148-161. https://doi.org/10.1016%2Fj.geotexmem.2015.01.001.

Rizzitano, S., Cascone, E. and Biondi, G. (2014), "Coupling of topographic and stratigraphic effects on seismic response of slopes through 2D linear and equivalent linear analyses", *Soil Dyn. Earthq. Eng*., **67**, 66-84. https://doi.org/10.1016/J.SOILDYN.2014.09.003.

Rodrıguez, C.E., Bommer, J.J. and Chandler, R.J. (1999), "Earthquake-induced landslides: 1980–1997", *Soil Dyn. Earthq. Eng.*, **18**(5), 325-346. https://doi.org/10.1016/S0267-7261(99)00012-3.

Somerville, P.G., Smith, N.F., Graves, R.W. and Abrahamson, N.A. (1997), "Modification of empirical strong ground motion attenuation relations to include the amplitude and duration effects of rupture directivity", *Seismol. Res. Lett.*, **68**(1), 199-222. https://doi.org/10.1785%2Fgssrl.68.1.199.

Song, J. and Rodriguez-Marek, A. (2015), "Sliding displacement of flexible earth slopes subject to near-fault ground motions". *J. Geotech. Geoenviron. Eng.*, **141**(3), 04014110. https://doi.org/10.1061%2F%28asce%29gt.1943-5606.0001233.

Ministry of Housing and Urban Rural Development of the People's Republic of China and State Administration for Market Regulation (2019), Standard for geotechnical testing method (GB/T 50123–2019), Beijing, China. (In Chinese)

Sun, P., Yin, Y.P., Wu, S.R. and Chen, L.W. (2012), "Does vertical seismic force play an important role for the failure mechanism of rock avalanches? A case study of rock avalanches triggered by the Wenchuan earthquake of May 12, 2008, Sichuan, China". *Environ. Earth Sci.*, **66**(5), 1285-1293. https://doi.org/10.1007%2Fs12665-011-1338-8

Sun, Z., Kong, L., Guo, A. and Tian, H. (2015), "Surface deformations and failure mechanisms of deposit slope under seismic excitation", *Rock Soil Mech*., **36**(12), 3465-3481. (In Chinese)

Wang, K.L. and Lin, M.L. (2011), "Initiation and displacement of landslide induced by earthquake-a study of shaking table model slope test", *Eng. Geol*., **122**(1-2), 106-114. https://doi.org/10.1016%2Fj.enggeo.2011.04.008.

Wen, Z., Xie, J., Gao, M., Hu, Y. and Chau, K.T. (2010), "Near-source strong ground motion characteristics of the 2008 Wenchuan earthquake", *Bull. Seismol. Soc. Am.*, **100**(5), 2425-2439.

Zarnani, S., El-Emam, M.M. and Bathurst, R.J. (2011), "Comparison of numerical and analytical solutions for reinforced soil wall shaking table tests", *Geomech. Eng*., **3**(4): 291-321. http://dx.doi.org/10.12989/gae.2011.3.4.291

Zhang, Y., Zhang, J., Chen, G., Zheng, L. and Li, Y. (2015), "Effects of vertical seismic force on initiation of the Daguangbao landslide induced by the 2008 Wenchuan earthquake", *Soil Dyn. Earthq. Eng.*, **73**, 91-102. https://doi.org/10.1016%2Fj.soildyn.2014.06.036.

Zhang, Y.B., Xiang, C.L., Che, Y.L., Cheng, Q.G., Xiao, L., Yu, P.C. and Chang, Z.W. (2019), "Permanent displacement models of earthquake-induced landslides considering near-fault pulse-like ground motions", *J. Mountain Sci.*, **16**(6), 1244-1257. https://doi.org/10.1007%2Fs11629-018-5067-2.

Zheng, L., Chen, G., Zen, K. and Kasama, K. (2012), "Numerical validation of Multiplex Acceleration Model for earthquake induced landslides", *Geomech. Eng.*, **4**(1), 39-53. https://doi.org/10.12989/gae.2012.4.1.039.